sciendo

Polish Journal of Chemical Technology, 22, 2, 50—55, 10.2478/pjct-2020-0016

Synthesis of antibacterial polyurethane film and its properties

Zhao Lin[1], Li Yunyun[1], Cheng Bin[2,*], Chen Yu[1]

[1]*School of Materials Science and Engineering, Beijing Institute of Technology, Beijing 100081, P. R. China*
[2]*Department of Clinical Laboratory, People's Hospital of Pudong New District, Shanghai 201200, P. R. China*
[*]*Corresponding authors: e-mail: 18300132@qq.com*

Polyurethane (PU) is a polymer widely used in the biomedical field with excellent mechanical properties and good biocompatibility. However, it usually exhibits poor antibacterial properties for practical applications. Efforts are needed to improve the antibacterial activities of PU films for broader application prospect and added application values. In the present work, two PU films, TDI-P(E-co-T) and TDI-N-100-P(E-co-T), were prepared. Silver nanoparticles (AgNPs) were composited into the TDI-N-100-P(E-co-T) film for better mechanical properties and antibacterial activities, and resultant PU/AgNPs composite film was systematically characterized and studied. The as-prepared PU/AgNPs composite film exhibits much better antibacterial properties than the traditional PU membrane, exhibiting broader application prospect.

Keywords: polyurethane, Ag nanoparticles, antibacterial, composite film.

INTRODUCTION

Polyurethane (PU) is a general term of the macromolecular compounds containing repeated carbamate groups (-NHCOO-) in the backbone chain. It is the product of the addition polymerization of polyisocyanate with oligomeric polyol. Due to its good comprehensive properties, such as diverse forms and properties, excellent strength and toughness, oil resistance, chemical corrosion resistance and so on, PU has been applied to the medical field as a dressing material[1, 2]. The backbone chain of hydroxy-terminated ethylene oxide tetrahydrofuran copolymer ether (P(E-co-T)) is composed of methylene ($-CH_2$) and ether bond (R-O-R) groups, which endows PU medical films good flexibility, excellent mechanical properties and environmental adaptability[3].

During the usage and storage, the surface of PU material is prone to grow and reproduce bacteria at appropriate temperatures and humidity because of its nutrient bases, which can break and decolor the material, and shorten the service life of the material[4]. In addition to the nutrient bases, various modification additives in PU material, such as plasticizers, stabilizers and fillers, can also serve as the nutrient sources of microorganisms. The nutrients provided by these additives allow bacteria to multiply to large numbers under suitable conditions and eventually deteriorate the PU material[5]. Improving the antibacterial activities of PU material is highly desired for broader application prospect and added application values.

For many years, scientists have committed to developing antibacterial agents and studying the antibacterial mechanism. Among various antibacterial agents, antibiotics possess the best antibacterial properties, yet are easily subject to drug resistances[6]. Most of organic antibacterial agents, such as quaternary ammonium salt, perform poorly upon the broad-spectrum antibacterial activities. ZnO nanoparticles have been successfully composited into a PU film to improve its antibacterial properties. However, the antibacterial activity is significantly affected by light irradiation[7, 8].

Ag is an important inorganic antibacterial agent that can destroy the inherent components or cause functional disorder and even death of bacteria upon contacts[9, 10]. It can also catalyze and activate the reaction of water with the oxygen in air to produce hydroxyl radicals (·OH) with strong oxidizing ability and reactive oxygen ion (O^{2-}) under light irradiation to enhance the sterilization ability[11, 12]. In addition, Ag antibacterial agents are low toxic, strongly antibacterial and easy to be composited with a variety of matrixes. Several composites of Ag and PU have been prepared by simply combining Ag with PU. For example, Wang *et al.*[13] fabricated a PU/keratin nanofibrous by electrostatic spinning. Ag nanoparticles (AgNPs) were *in situ* composited into the nanofibrous to form a novel nanofibrous composite mat. The mat exhibited better biocompatibility, antibacterial properties and wound healing performance, as compared with the conventional gauze sponge dressings. Prashant *et al.*[14] obtained a uniformly coated PU foam by immersing a PU foam in nanosilver solution overnight. The nanosilver coated PU foam was test for water filtration using *E. coli* as the water pollution index. No bacteria were detected in the output water due to the excellent antibacterial ability of the foam. However, these methods rarely produce the composites directly during the preparation of PU. P(E-co-T) is a class of polyether prepolymers with good flexibility and low glass transition temperatures[15]. The PUs prepared from P(E-co-T) also possess good flexibility, good low temperature mechanical properties and excellent environmental adaptability[16]. In the present work, AgNPs were directly dispersed in P(E-co-T) by physical mixing method, and then subjected to the one pot reaction to yield PU/AgNPs composite films. The properties of the composite films were systematically characterized and analyzed.

EXPERIMENTAL

Materials

P(E-co-T) (hydroxyl value, 25.2 mg KOH/g) of chemical grade was obtained from Luoyang Liming Chemical Industry Research Institute (Luoyang, China) and was dried in a vacuum oven at 60°C for 2 h before use. Analytical grade toluene-2, 4-diisocyanate (TDI) and polyfunctional urea-isocyanate (N-100) were purchased from Luoyang Liming Chemical Industry Research Institute and stored

in a desiccator before use. The molar ratio of 2,4-isomer to 2,6-isomer of TDI is 8:2 and the -NCO content of N-100 is 22.0±0.3%. Dibutyltin dilaurate (T-12) and triphenylbismuth (TPB) (analytical grade) were supplied by Beijing Chemical Reagent Co., Ltd (Beijing, China). They were respectively dissolved in dibutyl phthalate to form 1.5 wt% solutions. AgNPs with the purity of 99.5% and average particle size of 120 nm were purchased from Shanghai Aladdin Reagent Co., Ltd (Shanghai, China). Analytical grade dibutyl phthalate was obtained from Beijing Chemical Factory (Beijing, China).

Preparation of PU film

Twenty grams of P(E-co-T) were added into a three-necked flask that was pre-purged with nitrogen to remove water vapor and stirred at the constant temperature of 85°C for 30 minutes. A certain amount of TDI or the mixture of TDI and N-100 was added into the flask at the desired [-NOC]/[-OH] ratios (R) and stirred for 1 h. The composition of each experimental sample is shown in Table 1. Catalyst T-12 and TPB were then added into the flask and stirred for 30 min. The resultant product was vacuumed to remove bubbles, poured into a polytetrafluoroethylene (PTFE) mold, vacuumed until no new bubbles appeared and solidified in an oven at 75°C for 7 days to obtain a PU film.

Synthesis of TDI-N-100-P(E-co-T)PU/AgNPs film

AgNPs (0.2 g, 0.5 wt%) were dispersed into dibutyl phthalate (8 g, 20 wt%). The suspension was mixed with P(E-co-T) polyether at 85°C under the protection of nitrogen atmosphere in a 100 mL three-mouth flask and stirred for 30 min. TDI/N-100 was added to the flask and the mixture was stirred for 1 h. Catalysts T-12 and TPB were then added into the flask and stirred for 30 min. The composition of each sample is shown in Table 1. The resultant product was vacuumed to remove bubbles, poured into a PTFE mold, vacuumed again until no new bubbles appeared and solidified in an oven at 75°C for 7 days to form a TDI-N-100-P(E-co-T) PU/AgNPs film.

Characterizations

FTIR measurements were performed with a NEXUS-470 FTIR infrared spectrometer (Nicolet company, USA) in the scanning range of 500–4000 cm^{-1} using KBr pellets. The XRD patterns of the as-prepared PU films were recorded on an X-ray diffractometer (XRD-6000. Shimadzu company, Japan) using CuKα radiation (wavelength $\lambda = 0.154$ nm) at the voltage of 40 kV and the current of 30 mA in the scanning range from 10° to 50°. The scanning rate was set to 5 °/min. The glass transition temperature of each film product was determined by DSC using a DSC200PC differential scanning calorimeter (NETZSCH company, Germany) at the heating rate of 5°C/min from –100°C to –20°C. PU film samples were respectively mounted on a metal stub with a conductive tape, sputter-coated with a thin layer of gold and imaged under a scanning electron microscope (Hitachi X650, Japan) for the dispersion of AgNPs.

The mechanical properties of each sample were tested according to the GB/T528-92 standard. The samples were respectively cut into 20 mm long, 5mm wide and ~1mm thick dumbbell-shaped specimens. Stress-strain curve was measured with an Instron 6022 series material testing machine at the strain rate of 100 mm/min and temperature of 25°C. The maximum tensile strength (σ_m (MPa)), maximum elongation (ε_m (%)) and elongation at break (ε_b (%)) of each sample were obtained from the stress-strain curve. Each test was repeated five times and the mean value was reported.

The antibacterial efficacy of TDI-N-100-P(E-co-T) PU/AgNPs film was evaluated with Gram negative E. coli ATCC 25933 by the zone of inhibition test. The bacterial species on an inclined surface were selected and shaken in sterile water with glass beads for several minutes to obtain a suspension of baceria. An aliquot of 0.1 mL suspension was uniformly dispersed on a cured luria-bertani medium under aseptic operation. The sample with the diameter of 3 cm was disinfected by ultraviolet light, placed in the medium and cultivated at 37°C for 18 h. The bacteriostatic circle around the sample was imaged.

RESULTS AND DISCUSSION

Characterizations of PU film

The TDI-N-100-P(E-co-T) PU film was first characterized by FTIR. The reaction between isocyanate monomer and P(E-co-T) produces a carbamate ester group (-NH-CO-O-). The stretching vibration and bending vibration of N-H are observed at 3433.59 cm^{-1} and 3433.59 cm^{-1}, respectively (Fig. 1). The film also exhibit a peak at 1729.38 cm^{-1} due to the stretching vibration of C=O. No peak of the -NCO is found at 2270 cm^{-1} on the spectrum, indicating that TDI and N-100 have been completely reacted.

The stress-strain curves of TDI-P(E-co-T) PU and TDI-N-100-P(E-co-T) PU films prepared at different

Table 1. Compositions of experimental samples

Film type	No.	R value	Molar raio of TDI/N-100	Mass content of AgNPs
TDI-P[E-co-T]	TP-1	1.20	–	–
	TP-2	1.30	–	–
	TP-3	1.41	–	–
	TP-4	1.50	–	–
	TP-5	1.65	–	–
TDI-N-100-P[E-co-T]	TNP-1	1.38	0.8/0.2	–
	TNP-2	1.50	0.8/0.2	–
	TNP-3	1.63	0.8/0.2	–
	TNP-4	2.62	0.8/0.2	–
TDI-N-100-P[E-co-T]/AgNPs	TNP/AgNPs-1	1.50	0.8/0.2	0
	TNP/AgNPs-1	1.50	0.8/0.2	0.5
	TNP/AgNPs-1	1.50	0.8/0.2	1.0
	TNP/AgNPs-1	1.50	0.8/0.2	1.5

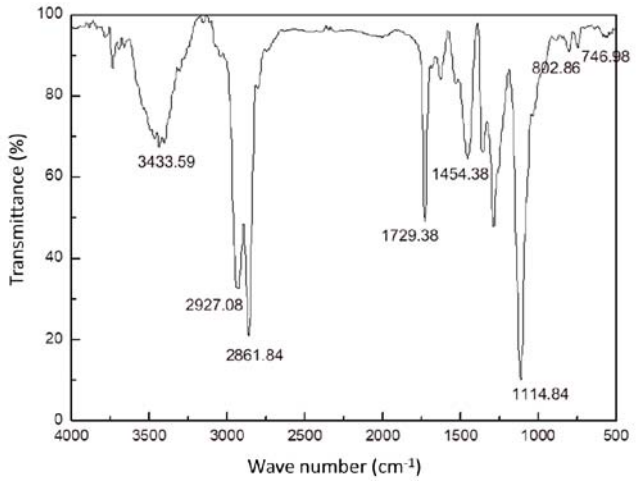

Figure 1. FTIR spectrum of TDI-N-100-P(E-co-T) film

[-NOC]/[-OH] ratios (R) were first meausred. Figure 2 shows the effects of R on the maximum tensile strength (σ_m) and the elongation at break (ε_b). The σ_m of TDI--P(E-co-T) PU film gradually increases and its ε_b first increases and then decreases with the increase of R. It can be explained that more -NCO groups react with the -OH in P(E-co-T) at high -NCO contents under same conditions[17], and more carbamate ester groups are form. Therefore, both σ_m and ε_b gradually increase. Increasing the -NCO content results in higher contents of hard segment in TDI-P(E-co-T) PU, which improves the strength and hardness of the film. Despite the good resilience of the soft segment, ε_b inevitably decreases as the content of soft segment in the film is decreased. In addition, excessive –NCO can react with carbamate ester to form urea formate ester, causing chemical cross-linking that inhibits chain extension reaction and reduces chain extension efficiency, and thus also decreases the elongation at break. In all, the TDI-P(E-co-T) PU films prepared at the R values between 1.4 and 1.5 can exhibit relatively good mechanical properties and good extensibility. The maximum tensile strength and elongation at break of the TDI-N-100-P(E-co-T) PU film exhibits similar changing trends with the increase of hard segment content to those of TDI-P(E-co-T) PU film (Fig. 2b). Due to the introduction of N-100 containing the trifunctional group, the ε_b of TDI-N-100-P(E-co-T) PU film is lower than that of TDI-P(E-co-T) PU film.

The crystallinity of the TDI-P(E-co-T) and TDI-N--100-P(E-co-T) PU films with different hard segment contents was determined by XRD. The TDI-P(E-co-T) film cured with TDI contains more regular hard segments and thus exhibits higher crystallinity than the film cured with N-100 due to the asymmetry of N-100 (Fig. 3). In

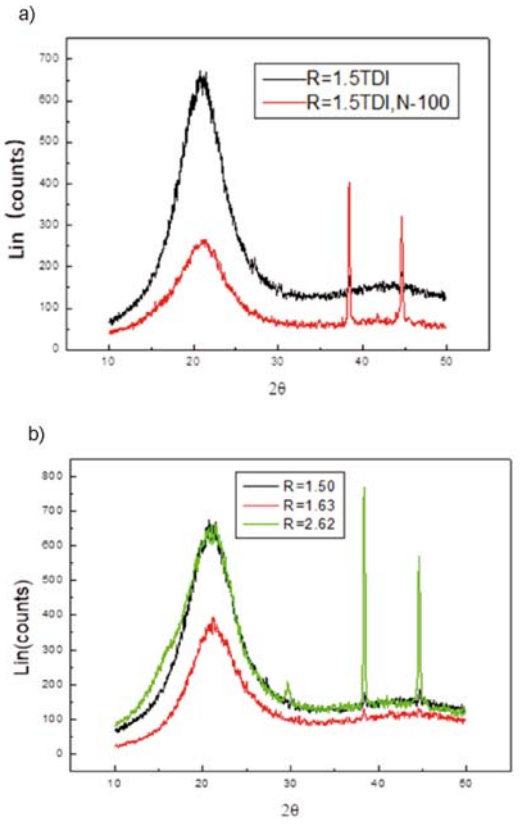

Figure 3. XRD patterns of TDI-P(E-co-T) and TDI-N-100 PU films (a) and the TDI-P(E-co-T) PU films with different hard segment contents (b)

addition, the crystallization degrees of both PU films increase first and then decrease with the increase of hard segment content. The hard segment cannot be crystallized or crystallized very slowly at low contents. The formation of an orderly arranged concentrated hard segment area out of soft segments is a very slow process, and the hydrogen bonding interaction between the hard and soft segments also hinders such ”separation”. The degree of aggregation between hard segments increases with the increase of content, and the effects of hydrogen

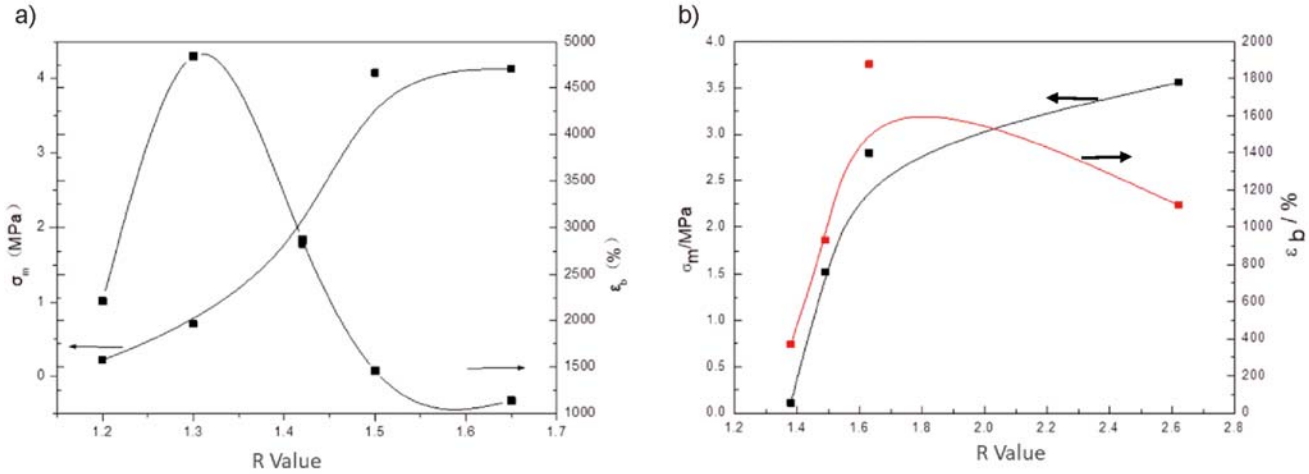

Figure 2. Mechanical properties of TDI-P(E-co-T) PU (a) and TDI-N-100-P(E-co-T) PU (b) films prepared at different R values

bonding are enhanced, resulting in the orderly accumulated hard segments and better crystallization. However, a large amount of hard segments can be mixed with the soft segments, which destroys the orderly stacked structure of soft segment and significantly reduces the crystallization degree[18, 19].

The glass transition temperatures (Tg) of the TDI--P(E-co-T) and TDI-N-100-P(E-co-T) films with different structures were determined by DSC. As shown in Figure 4 for their DSC curves, the TDI-P(E-co-T) and TDI-N-100-P(E-co-T) films prepared at the R of 1.5 exhibit the glass transition temperatures (Tg) of –79.8 and –78.1°C. The higher Tg of TDI-N-100-P(E-co-T) film is due to the its higher degree of crosslinking. The Tg of the TDI-N-100-P(E-co-T) film raises to –77.3°C as the R value increased to 1.63. These results suggest that higher R values of PU film result in higher Tg. The low Tg of the PU films prepared in the present work is due to the good flexibility of P (E-co-T) skeleton.

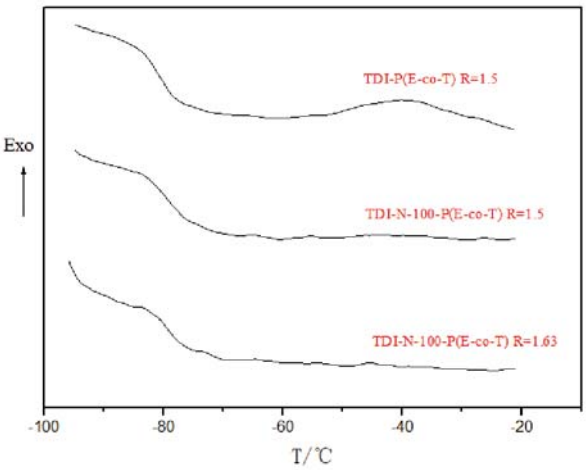

Figure 4. DSC curves of TDI-P(E-co-T) and TDI-N-100-P(E--co-T) films prepared under different conditions

Characterization of TDI-N-100-P(E-co-T)PU/AgNPs film

The distribution of AgNPs in PU film was imaged by SEM. Figure 5 shows the SEM images of TDI-N-100-P(E--co-T) PU film and the PU/AgNPs film containing 1% AgNPs. It is clear that the AgNPs are uniformly distributed in the TDI-N-100-P(E-co-T) PU film.

The tensile strengths and elongations at break of the PU/AgNPs films with different AgNPs contents were measured to evaluate their mechanical properties. The tensile strength of the composite film remains stable with the increase of AgNPs content up to 1.0% and dramatically decreases as the content of AgNPs further increased to 1.5% (Black line in Fig. 6). The elongation at break gradually increases with the increase of AgNPs content (Blue line in Fig. 6).

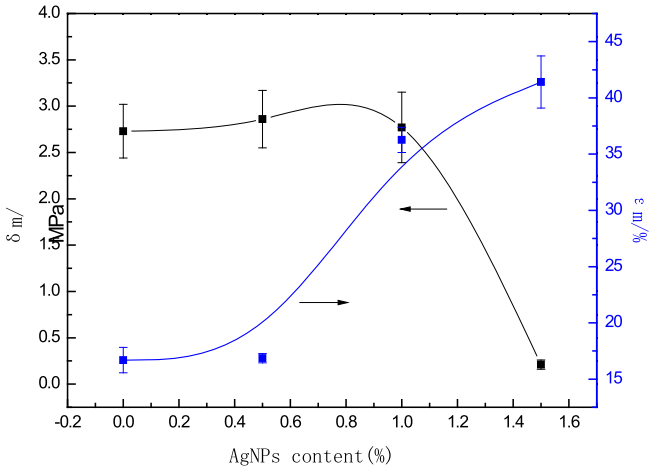

Figure 6. Mechanical properties of the PU/AgNPs films with different contents of AgNPs

The AgNPs in TDI-N-100-P(E-co-T) PU film can function as the reinforcing particles. They afford a certain load, absorb part of the energy accumulated from stress, and cause crack bifurcate or change the direction as an external force imposed on the film. Therefore, they can disperse stress, prevent the continued development of crack, delay fracture, and improve the mechanical properties of the material. Compositing the inorganic NPs during the preparation of TDI-N-100-P(E-co-T) PU can increase the confusion degree of the soft and hard segments in the PU matrix[20]. The chemical bonds or hydrogen bonds formed between the surface groups of AgNPs and the isocyanate group of TDI-N-100-P(E-co-T)

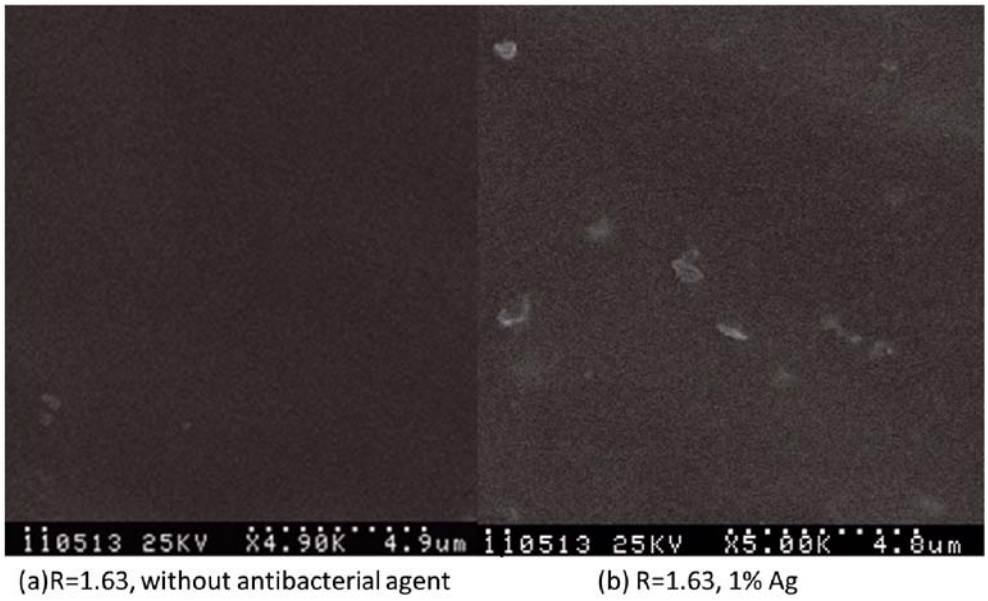

Figure 5. SEM images of TDI-N-100-P(E-co-T) PU film and the PU/AgNPs film containing 1% AgNPs

PU can facilitate the macromolecular crystallization, increase the hard segment content and improve the mechanical properties of the composite film[21]. In addition, external forces can cause the stress concentration effect around the AgNPs dispersed in the TDI-N-100-P(E-co-T) PU film to produce silver striations that can also absorb energy. Therefore, the composite films exhibit better toughness than PU film.

The antibacterial efficacy of the PU/Ag film was evaluated by the zone of inhibition test with the film samples containing no AgNPs and 0.5% AgNPs. Antibacterial circles are formed on the PU/AgNPs composite film containing 0.5% AgNPs and no obvious antibacterial circle is observed on the film containing no AgNPs (Fig. 7), suggesting the strong antibacterial activity of the composite film against E. coli. The positive Ag^+ and the negatively charged cytomembrane attract each other by Coulomb force, which adheres the bacteria onto the composite film surface. Ag^+ then penetrates the cytoderm into bacterial cells to inhibit the activity of cell synthase, and damages the microbial electronic transport system, respiratory system and material transfer system. Eventually the cells lose the ability to divide and multiply and die. The excellent antibacterial properties of PU/AgNPs composite film can significantly promote the application of PU film as a medical dressing material.

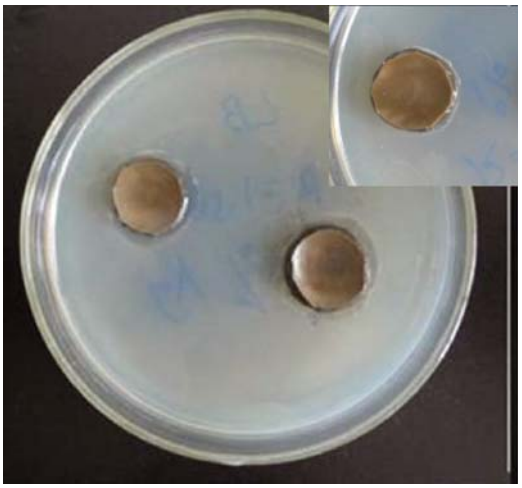

Figure 7. Antibacterial efficacy of the PU/Ag film containing 0.5% AgNPs and 0% AgNPs (insert image)

CONCLUSION

TDI-P(E-co-T) and TDI-N-100-P(E-co-T) PU films were respectively prepared and characterized for their structures, crystallization properties and mechanical properties. AgNPs were successfully composited with TDI-N-100-P(E-co-T) PU film *in situ* by one-pot reaction. The AgNPs are evenly dispersed in the composite film, and can enhance the tensile strength and elongation at break of the composite film. In addition, the AgNPs endow the film excellent antibacterial activity against E. coli. The PU/AgNPs composite film with the excellent antibacterial and mechanical properties can potentially improve the poor antibacterial property of PU medical membrane and have broad application prospect.

LITERATURE CITED

1. Engels, H., Pirkl, H., Albers, R., Albach, R.W., Krause, J., Hoffmann, A., Casselmann, H. & Dormish, J. (2013). Polyurethanes: versatile materials and sustainable problem solvers for today's challenges. *Angew. Chem. Int. Ed.* 52, 9422-9441.

2. Li, M., Chen, J., Shi, M.T., Zhang, H.L., Ma, P.X. & Guo, B.L. (2019). Electroactive anti-oxidant polyurethane elastomers with shape memory property as non-adherent wound dressing to enhance wound healing. *Chem. Eng. J.* 375, UNSP 121999.

3. Wang, Y., Wang, M.N., Zhao, X.H., Gao, Y. & Liu, M.X. (2017). Determination of antioxidant content in hydroxyl-terminated ethylene oxide-tetrahydrofuran copolyether using ultraviolet spectrophotometry. *Chem. Propell. Polym. Mater.* 15, 92–94.

4. Sun, M.F., Ren, X.E., Zhang, J.H., Zhang, X.M. & Wang, H.Y. (2019). Preparation and characterization of one-component polyurethane powder adhesives by the solution polymerization technology. *J. Appl. Polym. Sci.* 136, 47898.

5. Tsou, C., Lee, H., Hung, W., Wang, C., Shu, C., Suen, M. & De Guzman, M. (2016). Synthesis and properties of antibacterial polyurethane with novel bis(3-Pyridinemethanol) silver chain extender. *Polymer.* 85, 96–105.

6. Wekwejt, M., Michno, A., Truchan, K., Palubicka, A., Swieczko-Zurek, B., Osyczka, A. M. & Zielinski, A. (2019). Antibacterial activity and cytocompatibility of bone cement enriched with antibiotic, nanosilver, and nanocopper for bone regeneration. *Nanomaterials* 136, 47898.

7. Artifon, W., Pasini, S.M., Valerio, A., Gonzalez, S.Y. G., de Souza, S.M.D.G.U. & de Souza, A.A.U. (2019). Harsh environment resistant – antibacterial zinc oxide/Polyetherimide electrospun composite scaffolds. Mat. Sci. Eng. C-Mater. 103, 109859.

8. Kim, J.H., Ma, J., Lee, S., Jo, S. & Kim, C.S. (2019). Effect of ultraviolet-ozone treatment on the properties and antibacterial activity of zinc oxide sol-gel film. *Materials* 12, 2422.

9. Hu, Z.H., Zhang, L., Zhong, L.L., Zhou, Y.Z., Xue, J.Q. & Li, Y. (2019). Preparation of an antibacterial chitosan-coated biochar-nanosilver composite for drinking water purification. *Carbohyd. Polym.* 219, 290–297.

10. Dil, N.N. & Sadeghi, (2019). M. Free radical synthesis of nanosilver/gelatin-poly (acrylic acid) nanocomposite hydrogels employed for antibacterial activity and removal of Cu(II) metal ions. *J. Hazard. Mater.* 351, 38–53.

11. Jaffari, Z.H., Lam, S.M., Sin, J.C. & Zeng, H.H. (2019). Boosting visible light photocatalytic and antibacterial performance by decoration of silver on magnetic spindle-like bismuth ferrite. *Mat. Sci. Semicon. Proc.* 101, 103–115.

12. Yu, N.X., Cai, T.M., Sun, Y., Jiang, C.J., Xiong, H., Li, Y.B. & Peng, H.L. (2018). A novel antibacterial agent based on AgNPs and Fe_3O_4 loaded chitin microspheres with peroxidase-like activity for synergistic antibacterial activity and wound-healing. *Int. J. Phar.* 552, 277–287.

13. Wang, Y., Li, P., Xiang, P., Lu, J., Yuan, J., & Shen, J. (2016). Electrospun polyurethane/keratin/agnp biocomposite mats for biocompatible and antibacterial wound dressings. *J. Mater. Chem. B.* 4, 635–648.

14. Jain, P. & Pradeep, T. (2005). Potential of silver nanoparticle-coated polyurethane foam as an antibacterial water filter. *Biotechnol. Bioeng.* 90, 59–63.

15. Lan, Y.H., Li, D.H., Zhai, J.X. & Yang, R.J. (2015). Molecular dynamics simulation on the binder of ethylene oxide-tetrahydrofuran copolyether cross-linked with N100. *Ind. Eng. Chem. Res.* 54, 3563–3569.

16. Zhai, J.X., Qu, Z.Y., Zou, Y.C., Guo, X.Y. & Yang, R.J. (2015). Study on preparation and properties of polyether polytriazole elastomers. *Chinese J. Polym. Sci.* 33, 597–606.

17. Madhavan, K. & Reddy B.S.R. (2006). Synthesis and characterization of poly(dimethylsiloxane-urethane) elastomers:

Effect of hard segments of polyurethane on morphological and mechanical properties. *J. Polym. Sci. Pol. Chem.* 44, 2980–2989.

18. Stribeck, A., Eling, B., Poselt, E., Malfois, M. & Schander, E. (2019). Melting, solidification, and crystallization of a thermoplastic polyurethane as a function of hard segment content. Macromol. Chem. Phys. 220, 1900074.

19. Wang, F.F., Chen, S.L., Wu, Q., Zhang, R.C. & Sun, P.C. (2019). Strain-induced structural and dynamic changes in segmented polyurethane elastomers. *Polymer* 163, 154–161.

20. Fang, H.G., Wang, H.L., Sun, J., Wei, H.B. & Ding, Y.S. (2016). Tailoring elastomeric properties of waterborne polyurethane by incorporation of polymethyl methacrylate with nanostructural heterogeneity. *RSC. Adv.* 6, 13589–13599.

21. Wu, G.M., Liu, G.F., Chen, J. & Kong, Z.W. (2017). Preparation and properties of thermoset composite films from two-component waterborne polyurethane with low loading level nanofibrillated cellulose. *Prog. Org. Coat.* 106, 170–176.